ChemComm

COMMUNICATION

View Article Online
View Journal | View Issue

Template-assisted *in situ* polymerization for forming blue organic light-emitting nanotubes†

Cite this: *Chem. Commun.*, 2014, **50**, 8208

Received 13th March 2014,
Accepted 3rd June 2014

DOI: 10.1039/c4cc01877j

www.rsc.org/chemcomm

Li-Chi Lee,[a] Han Han,[a] Yu-Tang Tsai,[b] Gang-Lun Fan,[a] Hsiang-Fang Liu,[a] Chung-Chih Wu,*[b] Jing-Jong Shyue,[c] Shih-Sheng Sun,[d] Chien-Liang Liu,[a] Pi-Tai Chou[a] and Ken-Tsung Wong*[a]

A functional monomer was thermally polymerized inside the anodized aluminum oxide (AAO) channel into nanotubes, which were isolated and characterized to be semiconductive and blue fluorescent, and were utilized as nano-containers of Fe_3O_4 nanoparticles to form magnetic nanocomposites.

Recent advances in the interdisciplinary study of polymers with nanostructures have transformed fundamental research into practical applications. Particularly, one-dimensional (1-D) conjugated polymeric nanomaterials, with high aspect ratios, often induce photonic and electronic anisotropy that may be useful for realizing polarized emission and high charge mobility. As such, 1-D semiconductive polymers have been extensively studied for optoelectronic devices such as field effect transistors,[1] organic solar cells,[2] and organic light-emitting diodes (OLEDs).[3] A variety of synthetic strategies have been developed for preparing organic 1-D nanostructures, including self-assembly,[4] electrospinning,[5] nanolithography,[6] and physical vapor deposition.[7] In addition, porous anodized aluminum oxide (AAO) membranes were adopted as templates to guide the growth of 1-D nanomaterials.[8] Using the template-wetting technique, AAO membranes can be utilized as nanomolds for forming small-molecules or polymer nanowires[9] or nanotubes.[10] However, these linear organic nanostructures may have low tolerance of organic solvents. Alternatively, the nanotubes formed by *in situ* polymerization with AAO templates possess covalently linked networks, thus exhibiting strong resistance against organic solvents. For example, AAO can serve as the nanoreactor for electrodeposition of electro-active monomers to yield highly conductive polymers, such as polypyrrole, polythiophene, and polyaniline.[11] Yet more AAO-templated *in situ* polymerization for nanomaterials, such as [4+4] photocycloaddition of monomers with anthracene groups for nanorods,[12] metal-catalyzed polymerization of styrene for polystyrene nanofibrils,[13] and thermal cross-linking of triphenylamine derivatives for nanoarrays,[14] has been reported. One crucial advantage of AAO-templated *in situ* polymerization is that the designated function(s) can be implanted on the monomer, rendering the preparation of functional nanotubes feasible. In this work, we expand the scope of AAO-templated *in situ* polymerization to make blue fluorescent semiconductive nanotubes using a precursor featuring a hole-transport (HT) core and two polymerizable styryl pendants. The hollow nanotubes can be further filled with Fe_3O_4 nanoparticles to make light-emitting magnetic nanocomposites.

Scheme 1 depicts the chemical structure of the functional monomer (**VB-FNPD**), which has been previously used to produce high solvent tolerance and high-hole-mobility HT films for organic light-emitting devices (OLEDs) through thermal polymerization.[15] In **VB-FNPD**, the diarylamino groups attached to a rigid and planar fluorene core give the monomer efficient blue fluorescence. In addition, the polymerizable styryl groups were attached to the HT-active core *via* an inert sp^3-hybridized carbon bridge to preserve the functionalities of monomer cores after thermal polymerization.

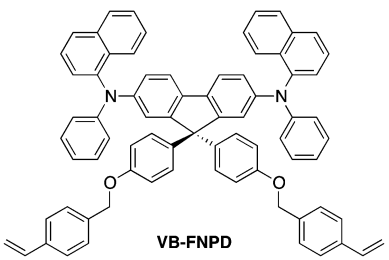

Scheme 1 The structure of **VB-FNPD**.

[a] *Department of Chemistry, National Taiwan University, Taipei 10617, Taiwan. E-mail: kenwong@ntu.edu.tw*
[b] *Department of Electrical Engineering, Graduate Institute of Electro-optical Engineering and Graduate Institute of Electronics Engineering, National Taiwan University, Taipei 10617, Taiwan. E-mail: wucc@ntu.edu.tw*
[c] *Research Center for Applied Sciences, Academia Sinica 128 Academia Road, Nankang, Taipei 115, Taiwan*
[d] *Institute of Chemistry, Academia Sinica 128 Academia Road, Nankang, Taipei 115, Taiwan*

† Electronic supplementary information (ESI) available: The UV-Vis absorption and photoluminescence spectra, the procedures for preparing the individual nanotubes, the nanotube arrays, the Fe_3O_4NP–blue-OLET nanocomposites, and the devices for electronic properties as well as the video for mechanical behavior. See DOI: 10.1039/c4cc01877j

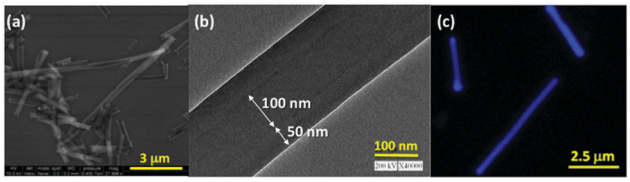

Fig. 1 Representative (a) SEM, (b) TEM, and (c) CLSM images of poly-**VB-FNPD** nanotubes.

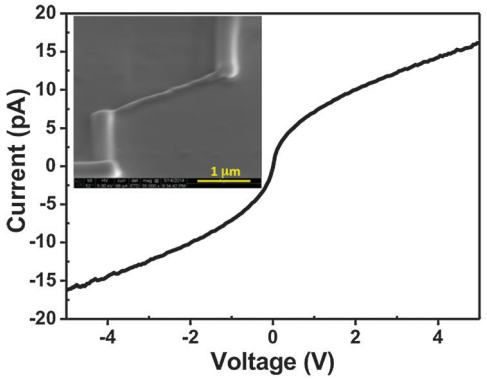

Fig. 2 Current–voltage (*I*–*V*) characteristics of the poly-**VB-FNPD** nanotube. The inset shows the SEM image of the nano device fabricated using a focus ion beam.

The polymeric nanotubes were achieved by combining the template wetting and *in situ* thermal polymerization (Scheme S1, ESI†), which were then dispersed in ethanol for further characterization.

The morphologies of the thermally cross-linked poly-**VB-FNPD** nanotubes were characterized by SEM and TEM. The SEM image (Fig. 1a) of the sonication-dispersed nanotubes shows the average outer diameter of ~200 nm, corresponding nicely to the inner diameter of the AAO template channels. The lengths of nanotubes range from several to tens of micrometers. The variations in lengths could be attributed to the ultrasonication and/or centrifugation-induced cracking of defected nanotubes, perhaps associated with incomplete coverage of the monomer solution over the AAO channels, the structural defects (branching), and the length variations of the AAO channels. The SEM image also indicates that exterior surfaces of nanotubes appear to be smooth and uniform. Meanwhile, the TEM image (Fig. 1b, also Fig. S1 in ESI†) clearly reveals a pair of internal surfaces inside external surfaces, confirming the tubular nature of formed nanostructures and implying the potential for further modification. The TEM images also reveal the wall thickness to be about 25–50 nm, depending on the section location on the tube (*e.g.*, near the tube end or center *etc.*) and AAO template properties.

The electronic absorption and photoluminescence (PL) spectra of nanotubes cast on a quartz slide show limited changes as compared to those of the monomer and thermally polymerized poly-**VB-FNPD** thin films (Fig. S2 in ESI†). The PL quantum yields of poly-**VB-FNPD** nanotubes are 0.12 and 0.05 in EtOH and films, respectively, which are comparable to those of monomers (0.15 in EtOH, 0.07 in films). These results reveal the effectiveness of the molecular design strategy by introducing the polymerizable styryl groups onto the sp^3-hybridized carbon bridge to preserve the photophysical properties of the active chromophore core after the polymerization. The luminescence of the individual poly-**VB-FNPD** nanotube was probed by confocal laser scanning microscopy (CLSM) (Fig. 1c). As shown, the well-dispersed nanotubes were clearly identified for their clear contours and strong blue fluorescence.

For probing the mechanical behavior (stiff or flexible) of the poly-**VB-FNPD** nanotubes, we used a homemade nano-manipulator which combines a scanning probe microscope (SPM) with an inverted optical microscope (OM). The nanotube sample (in EtOH) was drop-cast onto a microscope slide (18 × 18 mm). Then, the nanotubes were imaged using OM with an objector (100×), and manipulated using the SPM tip (radius 50 nm). As shown in the supporting video (see ESI†), one of the cast nanotubes was initially bent. As the SPM tip landed in physical contact with the sample, by controlling the PZT stage, the initially bent nanotube can be deformed using the SPM tip into a linear one, showing the flexibility of poly-**VB-FNPD** nanotubes.

Monomer **VB-FNPD** derived from the well-known HT material α-NPD should inherit the HT behavior of α-NPD. Therefore, the poly-**VB-FNPD** nanotube is expected to possess reasonable electrical conductivity. To probe the electronic behavior, the nano device (inset of Fig. 2) was fabricated by using focused-ion-beam (FIB) to make Pt contact with the nanotube between two ITO electrodes (Scheme S2 in ESI†). The representative *I*–*V* curve shown in Fig. 2 reveals a quasi-linear characteristic at the bias voltage from −5 to 5 V. The extracted device resistance $R_{\text{VB-FNPD}}$ is *ca.* 5.0×10^{11} Ω. With the measured nanotube length $L \sim 2.2$ μm, mean outer diameter $D \sim 200$ nm, and wall thickness $W \sim 25$–50 nm, the calculated nanotube resistivity $\rho = \pi R[D^2 - (D - 2W)^2]/4L \sim 1.8$–$3.1 \times 10^5$ Ω cm and the conductivity $\sigma \sim 3.2$–5.6×10^{-6} S cm^{-1}, which is of similar magnitude to other reported polymer nanowires.[16] The other nano devices employing nanotubes with various lengths exhibited comparable conductivities (see Fig. S3, ESI†), which are two orders higher than that of a monomer film (Scheme S3 and Fig. S4, ESI†).

The protocol combining template-wetting and *in situ* thermal polymerization followed by the removal of the template and sonicated dispersion renders possible not only the preparation of individual 1-D nanotubes, but also the ordered nanotube arrays with the support of transparent and flexible polystyrene substrates.[17] Before being subjected to de-templation in aqueous KOH, the nanotube-implanted AAO membrane was pressed on a pre-heated (230 °C) melt polystyrene (PS) (Scheme S4 in ESI†). After cooling to room temperature, the PS-supported AAO membrane was immersed in a 1 M KOH aqueous solution under sonication to remove the template. The SEM images (Fig. 3) clearly demonstrate that the poly-**VB-FNPD** nanotubes were successfully aligned, forming densely packed nanoarrays on top of polystyrene. The nanoarrays should approximately replicate the dimensions of the AAO channels with the estimated density of about 10^9 tubes per square centimeter and a mean height of about 50 μm. Since the nanotube is semiconductive and fluorescent, such nanoarrays may find potential applications in waveguides or

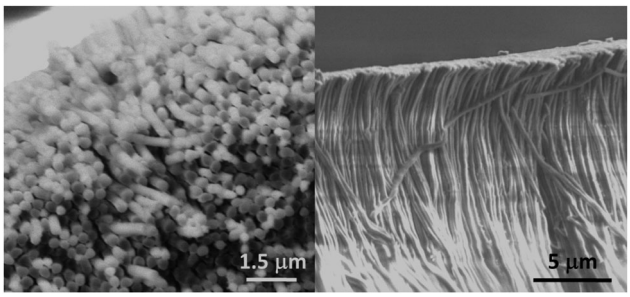

Fig. 3 SEM images of the array of poly-**VB-FNPD** nanotubes.

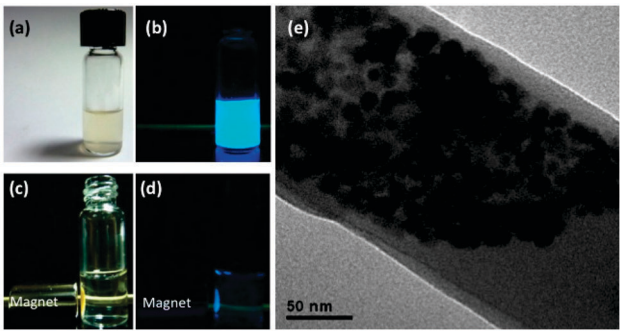

Fig. 4 (a) The Fe_3O_4NP–OLET nanocomposites dispersed in DI water. (b) The corresponding blue emission excited using a 365 nm UV lamp. (c) The nanocomposites attracted to one side of the vial by a magnet and (d) excited by UV. (e) The TEM image of Fe_3O_4NP–OLET nanocomposites.

microelectronics, for which the size and density of nanotubes can be customized by tailoring the AAO template.

Employing their hollow nature and the post wetting strategy, our organic light-emitting nanotubes (OLETs) can be utilized as nanocontainers to prepare nanocomposites with intriguing dual functions. Before removal of the template, the nanotube-implanted AAO membrane was impregnated with magnetic Fe_3O_4 nanoparticles (Fe_3O_4NP) (oleylamine/oleic acid capped, 12 ± 1 nm, in ethanol), facilitated by an external magnetic field (Scheme S5 in ESI†). The TEM image (Fig. 4e also Fig. S4 in ESI†) clearly reveals the Fe_3O_4 nanoparticles introduced into and aggregating inside the nanotubes that were removed from the template. The bifunctional behavior of the Fe_3O_4NP–OLET nanocomposites is clearly demonstrated in Fig. 4a–d. The aqueous solution of the dispersed magnetic nanocomposites (Fig. 4a) exhibited a strong blue emission under 365 nm UV light excitation (Fig. 4b). In the presence of a magnet (Fig. 4c), the nanocomposites were driven/located near the vial wall so that under UV excitation emission was observed only near the bottle rim. Such dual emission and positioning capabilities of the magnetic blue fluorescent OLETs may find some intriguing applications, *e.g.* bio-applications.[18]

In summary, a functional monomer **VB-FNPD** derived from the well-known HT material α-NPD was utilized to make organic light-emitting poly-**VB-FNPD** nanotubes by virtue of AAO-assisted template-wetting and *in situ* thermal polymerization. The new poly-**VB-FNPD** nanotubes were characterized using SEM, TEM, and CLSM, showing their hollow nature and intense blue fluorescence. Furthermore, the nanotubes exhibit mechanical flexibility and semi-conductivity as characterized by a nano-manipulator and a nano device fabricated by FIB, respectively. The nanotubes can be filled with Fe_3O_4 nanoparticles to prepare magnetic light-emitting nanotubes, giving new nanocomposites positioning capability with magnetic forces. The isolation of polymerizable styryl groups from the fluorescence- and HT-active chromophore core is the key feature for the nanotubes to preserve the optical properties of the monomer. Our established method shall allow one to make nanotubes with desired functions by tailoring the designated monomer in advance.

Notes and references

1 H. Sirringhaus, P. J. Brown, R. H. Friend, M. M. Nielsen, K. Bechgaard, B. M. W. Langeveld-Voss, A. J. H. Spiering, R. A. J. Janssen, E. W. Meijer, P. Herwig and D. M. de Leeuw, *Nature*, 1999, **401**, 685.
2 C.-Y. Chang, C.-E. Wu, S.-Y. Chen, C. Cui, Y.-J. Cheng, C.-S. Hsu, Y.-L. Wang and Y.-F. Li, *Angew. Chem., Int. Ed.*, 2011, **50**, 9386.
3 (*a*) B. O'Connor, K. H. An, Y. Zhao, K. P. Pipe and M. Shtein, *Adv. Mater.*, 2007, **19**, 3897; (*b*) Q. Niu, Y. Zhou, L. Wang, J. Peng, J. Wang, J. Pei and Y. Cao, *Adv. Mater.*, 2008, **20**, 964; (*c*) V. Vohra, U. Giovanella, R. Tubino, H. Murata and C. Botta, *ACS Nano*, 2011, **5**, 5572.
4 C. Giansante, G. Raffy, C. Schäfer, H. Rahma, M.-T. Kao, A. G. L. Olive and A. D. Guerzo, *J. Am. Chem. Soc.*, 2011, **133**, 316.
5 H. Yang, C. R. Lightner and L. Dong, *ACS Nano*, 2012, **6**, 622.
6 A. Del Campo and E. Arzt, *Chem. Rev.*, 2008, **108**, 911.
7 Y. S. Zhao, H. B. Fu, F. Q. Hu, A. D. Peng, W. S. Yang and J. N. Yao, *Adv. Mater.*, 2008, **20**, 79.
8 (*a*) S. J. Hurst, E. K. Payne, L. Qin and C. A. Mirkin, *Angew. Chem., Int. Ed.*, 2006, **45**, 2672; (*b*) M. R. Jones, K. D. Osberg, R. J. Macfarlane, M. R. Langille and C. A. Mirkin, *Chem. Rev.*, 2011, **111**, 3736; (*c*) Y. Liu, J. Goebl and Y. Yin, *Chem. Soc. Rev.*, 2013, **42**, 2610; (*d*) R. O. Al-Kaysi, T. H. Ghaddar and G. Guirado, *J. Nanomater.*, 2009, 436375; (*e*) J. Joo, K. T. Park, B. H. Kim, M. S. Kim, S. Y. Lee, C. K. Jeong, J. K. Lee, D. H. Park, W. K. Yi, S. H. Lee and K. S. Ryu, *Synth. Met.*, 2003, **235–236**, 7; (*f*) R. K. Zheng, H. L. W. Chan and C. L. Choy, *Nanotechnology*, 2005, **16**, 1928.
9 (*a*) D. O'Carroll, I. Lieberwirth and G. Redmond, *Small*, 2007, **3**, 1178; (*b*) L. Qu and G. Shi, *Chem. Commun.*, 2004, 2800.
10 (*a*) M. Steinhart, J. H. Wendorff, A. Greiner, R. B. Wehrspohn, K. Nielsh, J. Schilling, J. Choi and U. Gösele, *Science*, 2002, **296**, 1997; (*b*) M. Steinhart, R. B. Wehrspohn, U. Gösele and J. H. Wendorff, *Angew. Chem., Int. Ed.*, 2004, **43**, 1334; (*c*) S. Schlitt, A. Greiner and J. H. Wendorff, *Macromolecules*, 2008, **41**, 3228.
11 C. R. Martin, *Science*, 1994, **266**, 1961.
12 R. O. Al-Kaysi, R. J. Dillon, J. M. Kaiser, L. J. Mueller, G. Guirado and C. J. Bardeen, *Macromolecules*, 2007, **40**, 9040.
13 K. Y. Choi, J. J. Han, B. He and S. B. Lee, *J. Am. Chem. Soc.*, 2008, **130**, 3920.
14 (*a*) N. Haberkorn, J. S. Gutmann and P. Theato, *ACS Nano*, 2009, **3**, 1415; (*b*) N. Haberkorn, S. A. L. Weber, R. Berger and P. Theato, *ACS Appl. Mater. Interfaces*, 2010, **2**, 1573.
15 C.-Y. Lin, Y.-C. Lin, W.-Y. Hung, K.-T. Wong, R. C. Kwong, S. C. Xia, Y.-H. Chen and C.-I. Wu, *J. Mater. Chem.*, 2009, **19**, 3618.
16 G. A. O'Brien, A. J. Quinn, D. A. Tanner and G. Redmond, *Adv. Mater.*, 2006, **18**, 2379.
17 H. Watanabe and T. Kunitake, *Chem. Mater.*, 2008, **20**, 4998.
18 (*a*) S. J. Son, J. Reichel, B. He, M. Schuchman and S. B. Lee, *J. Am. Chem. Soc.*, 2005, **127**, 7316; (*b*) V. Kumar, G. Nath, R. K. Kotnala, P. S. Saxena and A. Srivastava, *RSC Adv.*, 2013, **3**, 14634.

